MethodsX xxx (2019) xxx–xxx

Contents lists available at ScienceDirect

MethodsX

journal homepage: www.elsevier.com/locate/mex

Method Article

A Multi Record Based Artificial Near Fault Ground Motion Generation Method

Zhen Liu[1,*], Shibo Zhang[1], Zhe Zhang[2]

[1] School of Management Science and Engineering, Shandong technology and business University, Yantai 264005 China
[2] School of Civil Engineering, Dalian University of Technology, Dalian, 116024, China

A B S T R A C T

Near fault ground motion is a kind of ground motion with great damage, which is difficult to simulate. The amplitude and frequency functions of near fault ground motion vary greatly with time. When a single ground motion is used for simulation, large errors can easily occur. A method for generating near fault ground motion based on a set of actual ground motions is presented. In order to evaluate these artificially near fault ground motions, artificial ground motions and corresponding natural ground motions are input into the finite element analysis program to obtain the response of the structure. It is found that these artificial near fault ground motions are good simulations of these actual ground motions. The method of near fault ground motion can make up for the shortage of near fault ground motion.

- Near Fault ground motions collected from the same earthquake with similar site characteristics are taken as sample group. Each ground motion in the sample group is considered as a record of random event.
- Because this method is based on multi ground motion samples, this method can take account of the variability of each ground motion sample on the premise of considering the earthquake characteristics, then the generated ground motion are more close to the real one.
- The wavelet technique and random vibration theory are applied to the analysis and simulation of ground motion. Because of the application of these two technologies, the simulation efficiency and accuracy of this method are improved.

A R T I C L E I N F O
Keywords: Artificial, ground motion, Velocity pulse, Chi-Chi earthquake, Wavelet, Near-fault
Article history: Received 2 July 2019; Accepted 31 October 2019; Available online xxx

* Corresponding author.
E-mail address: liuzhen1988@mail.dlut.edu.cn (Z. Liu).

https://doi.org/10.1016/j.mex.2019.10.036

Please cite this article in press as: Z. Liu, et al., A Multi Record Based Artificial Near Fault Ground Motion Generation Method, MethodsX (2020), https://doi.org/10.1016/j.mex.2019.10.036

Specification Table

Subject area	Engineering
More specific subject area	Artificial Ground Motion
Method name	Artificial Near Fault Ground Motion Generation Method
Resource availability:	NA

Background

Near fault ground motion is considered to be the most dangerous ground motion. Near fault ground motions generally occur near earthquake rupture faults. Near fault ground motions and far fault ground motions are significantly different [1,2], because near fault ground motions are believed to have the following characteristics : high PGV/PGA and PGD/PGA ratios, long-period velocity pulse and permanent ground displacements [3–5]. These characteristics are affected by fracture mechanism and fracture line direction. A large amount of energy is included in the long period velocity pulse, which will be input into the structure in a short time and then cause structural damage. The phenomenon of structural damage caused by near fault velocity pulses has recurred in the past several earthquakes [6].

Considering the safety of design, the final design of important structures is generally based on time history analysis [7,8]. Because the near fault ground motion is extremely destructive, it is difficult to simulate the destructive use of non near fault ground motion [9]. A large number of near fault ground motions are needed in time history analysis of important structures [10]. Comparing with non near fault ground motions, the number of near fault ground motions is very small. For example, over 3000 digital ground motions are obtained from the Chi-Chi earthquake by Taiwan Strong Motion Instrumentation Program which is operated by the Central Weather Bureau and cost about U.S. $40 million. Even in such seismic array, the near fault ground motions of the earthquake are relatively less. About 60 near fault ground motions are recorded in 20 km of the fault ruptures [11]. According to the classification of near fault motion ground [12–14], only 50 ground motions are considered to contain the velocity pulse. Because of this, only a few near fault motion grounds are available for many designs. To overcome this difficulty, many near fault ground motions which are recorded from locations other than the project site are selected and modified to match scale and spectrum. This change may produce some ground motions with unrealistic characteristics. For this reason, it is necessary to generate artificial near fault ground motions basing the real seismic data.

Method details

Artificial ground motion generation method

When natural ground motions can not meet the requirements of engineering, artificial seismic waves are needed to make up for them. With the deepening of the understanding of seismic properties and the application of new technologies to ground motion generation, many ground motion generation methods have been proposed.

The stationary filtering white noise model is proposed by Kanai and Tajimi [15,16] and is a very classic model. The artificial ground motion generation model has been developed and used by many researchers [17,18].

$$G(\omega) = Go\frac{1 + 4\xi_g^2\left(\frac{\omega}{\omega g}\right)}{\left(1 - \left(\frac{\omega}{\omega g}\right)^2\right)^2 + 4\xi_g^2\left(\frac{\omega}{\omega g}\right)^2} \tag{1}$$

G_o is constant power spectral intensity. ξ_g and ω_g are the site dominant damping coefficient and frequency, respectively. This artificial ground motion generation model has been widely used for a long time. But for technical reasons, the ground motion generation model has two serious problems:

Please cite this article in press as: Z. Liu, et al., A Multi Record Based Artificial Near Fault Ground Motion Generation Method, MethodsX (2020), https://doi.org/10.1016/j.mex.2019.10.036

First, the generated seismic waves are only related to the site characteristics and can not reflect the complexity of the ground motion. Second, the lack of simulation of the low frequency signals can not reflect the low frequency pulse [19]. At that time, the two problems were very difficult to solve. With the development of computer technology and signal analysis technology, there are many ways to solve these two difficulties such as wavelet analysis [19], artificial neural network or genetic algorithm.

In order to solve the first problem, a simulation method based on time-varying frequency and amplitude function is proposed by some researchers [20]. Seismic waves are considered to be generated by time-varying frequency functions and time-varying amplitude functions. This method considers that if the two functions of a ground motion are accurately obtained, the seismic waves generated by these two functions can be regarded as the simulation of the original seismic waves. To solve the second problem, a near fault ground motion identification method is proposed, which can be used to extract the velocity pulse in the near fault ground motion, so that the velocity pulse and the residue in the near fault ground motion can be simulated respectively [12].

The above two methods can be used to simulate a near fault ground motion. However, a ground motion record in an earthquake is only a sampling of the earthquake, which is equivalent to one random observation of the random process. The simulation of a single seismic record can not reflect the earthquake characteristics and magnify the bias in ground motion records. In this paper, a multi record based artificial ground motion generation method is proposed. This method regards ground motions recorded in a similar area as multiple sampling of the same random process. The artificial ground motion is generated by using the time-varying frequency and time-varying amplitude function obtained from multiple ground motions. This generation process can be divided into 5 steps. The first step is to select ground motion samples, which are from the same earthquake, and the nature of the site is similar. They can be considered as multiple sampling of the same random process. The second step is to extract velocity pulses from near fault ground motions. The existence of velocity pulse will affect the identification of time-varying frequency function and time-varying amplitude function by wavelet technology. For this reason, velocity pulses must be extracted before analysis. The third step is to obtain the time-varying and time-varying amplitude functions of each ground motion sample using wavelet technology. The fourth step is to use the mathematical method to estimate the two functions of the whole sample based on the time-varying frequency function and time-varying amplitude function of each ground motion. The fifth step is to use time-frequency function and time-varying amplitude function to generate artificial ground motion, and add the near fault velocity pulse extracted in the second step.

Near fault ground motion samples

To illustrate the method of ground motion generation based on multiple ground motions, the Chi-Chi earthquake in Taiwan will be used for simulation. The earthquake has obvious near fault effect and the earthquake stations are concentrated in Taiwan. Most of these earthquake stations are very advanced and have been corrected uniformly by the Central Weather Bureau, which makes these earthquake records have a uniform recording format and accuracy. In this paper, multiple records of an earthquake are regarded as multiple observations of a random event, so it is very important to ensure the uniformity of these records. Earthquake records from Taiwan can meet these requirements and reduce the error of this paper. In all Chi-Chi earthquake records, 50 records are considered to be near fault ground motions containing velocity pulses according to the Baker method and these ground motion records are listed in Table 1. Most of the records in the Table 1 are from TCU type earthquake stations, so the records of other types of earthquake stations will be excluded. Seismic waves vary when they propagate in space, so earthquakes need to be recorded in as small a range as possible to reduce the difference. For the above reasons, the 1182, 1193, 1244, 1402, 1403, 1462, 1464, 1470, 1471, 1472, 1473, 1475, 1514, 1523, 1524, 1525 1526 and 1595 earthquakes records were excluded.

Record Sequence Number is the number of the PEER; Tp-Pulse Period is the period of the extracted pulse using the method of the paper [12]; Rrup is the closest distance to rupture plane; Vs30 is average shear wave velocity of 30 meters deep.

It is found that all ground motion records are recorded in a small area near the epicenter, and the shear wave velocity of all sites is higher. This basically ensures the similarity of the recording site. The

Please cite this article in press as: Z. Liu, et al., A Multi Record Based Artificial Near Fault Ground Motion Generation Method, MethodsX (2020), https://doi.org/10.1016/j.mex.2019.10.036

Table 1
The details of the ground motions.

Record Sequence Number	Tp-Pulse Period (s)	Station Name	Rrup (km)	Vs30 (m/s)	PGAH (g)	PGAV (g)
1475	8.37	TCU026	56.12	569.98	0.10	0.05
1476	5.29	TCU029	28.04	406.53	0.20	0.06
1477	5.93	TCU031	30.17	489.22	0.11	0.07
1478	8.97	TCU033	40.88	423.40	0.16	0.07
1479	8.87	TCU034	35.68	393.77	0.25	0.07
1480	5.38	TCU036	19.83	478.07	0.13	0.06
1481	9.58	TCU038	25.42	297.86	0.14	0.07
1482	9.33	TCU039	19.89	540.66	0.20	0.12
1483	6.43	TCU040	22.06	362.03	0.12	0.08
1485	9.34	TCU045	26.00	704.64	0.51	0.18
1486	8.04	TCU046	16.74	465.55	0.36	0.27
1487	12.31	TCU047	35.00	520.37	0.22	0.18
1489	10.22	TCU049	3.76	487.27	0.24	0.11
1491	10.38	TCU051	7.64	350.06	0.45	0.20
1492	11.96	TCU052	0.66	579.10	0.18	0.12
1493	13.12	TCU053	5.95	454.55	0.14	0.09
1496	8.94	TCU056	10.48	403.20	0.17	0.05
1498	7.78	TCU059	17.11	272.67	0.16	0.13
1501	6.55	TCU063	9.78	476.14	0.12	0.08
1502	8.46	TCU064	16.59	645.72	0.79	0.26
1503	5.74	TCU065	0.57	305.85	0.51	0.53
1510	5.00	TCU075	0.89	573.02	0.26	0.23
1511	4.73	TCU076	2.74	614.98	0.43	0.21
1515	8.10	TCU082	5.16	472.81	0.19	0.10
1519	10.40	TCU087	6.98	538.69	0.11	0.09
1529	9.63	TCU102	1.49	714.27	0.26	0.13
1530	8.69	TCU103	6.08	494.10	0.14	0.15
1531	7.19	TCU104	12.87	410.45	0.10	0.09
1548	9.02	TCU128	13.13	599.64	0.16	0.09

sampling period and sampling duration of these records are same values, the sampling period and sampling duration are 0.005 s and 90 s, respectively.

It is necessary to extract near fault velocity pulses after obtaining the selected seismic samples. In this paper, Baker's method is used to extract the near fault velocity pulse [12]. Then the ground motion can be decomposed into two parts: velocity pulse and residual ground motion. Because of the strong experience of wavelet extraction method, different mother wavelets may have a great impact on the extraction results [21]. In order to obtain more complete velocity pulses, different mother wavelets are used to extract velocity pulses, and the results of 1476 seismic wave extraction are shown in the Fig. 1. According to the analysis of the extraction results, the 'db4' wavelet and 'db7' wavelet have good extraction effect for the selected seismic records. In this paper, 'db4' wavelet is used to extract velocity pulse.

After subtracting the large velocity pulse, the residual ground motion is obtained. Because the residual ground motion is a velocity time history, in order to get the time-varying amplitude function, the velocity time history is transformed to the acceleration time history.

The time-varying amplitude function

After obtaining these residual ground motions, the time-varying amplitude function and time-varying frequency function of each record can be obtained by using wavelet technology.

The first five these residual ground motions are shown as Fig. 2.

From Table 1, it can be found that the peak of each ground motion is different. Although the sampling conditions of the ground motion samples are similar in selecting ground motion, the number of seismic stations is limited and the epicentral distance between the stations is still different. To compensate for the effect of this deviation, the signal energy of all ground motion residual is adjusted

Please cite this article in press as: Z. Liu, et al., A Multi Record Based Artificial Near Fault Ground Motion Generation Method, MethodsX (2020), https://doi.org/10.1016/j.mex.2019.10.036

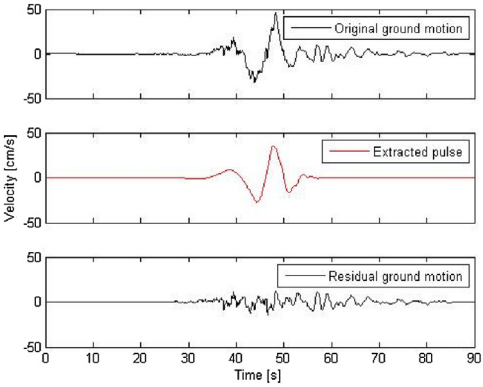

Fig. 1. The extracted largest velocity pulse.

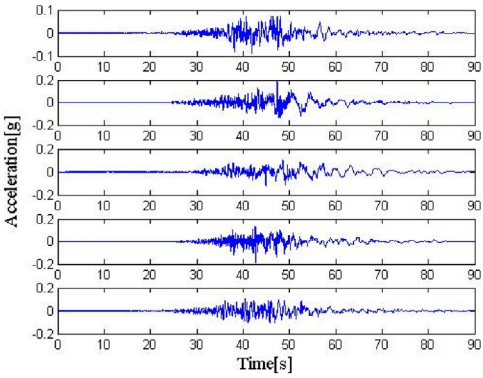

Fig. 2. Acceleration records of the ground motions.
(a) the horizontal component (b) the vertical component.

to a unified value. Then, the time-varying amplitude function of each sample is obtained by using wavelet technology, and the overall average time-varying amplitude function is shown as Fig. 3.

Many models can simulate time-varying amplitude functions. In order to better match the time-varying amplitude function obtained in this paper, the three segment function model is selected. The function model can be expressed as Formula 1

$$e(t) = \begin{cases} t/t_1 & 0 < t \le t_1 \\ 1 & t_1 < t \le t_2 \\ \exp[-\gamma(t - t_2)] & t_2 < t \le t_3 \end{cases} \tag{1}$$

where t_1 is the time that the acceleration record takes to reach its maximum value; t_2 is the duration time at which the acceleration keeps in its peak region; t_3 is the exponential decline time.

According to formula 1 and Fig. 3, the least square method is used to get formula 2 and

$$e(t) = \begin{cases} 1 \times 10^{-3} & 0 < t \le 15 \\ 1.1 \times 10^{-3}\left(t - 1.4 \times 10^{1}\right)^2 & 15 < t \le 35 \\ 4.9 \times 10^{-1} & 35 < t \le 46 \\ e^{\left(-t \times 6.7 \times 10^{-2} + 2.4\right)} & 46 < t \le 90 \end{cases} \tag{2}$$

Please cite this article in press as: Z. Liu, et al., A Multi Record Based Artificial Near Fault Ground Motion Generation Method, MethodsX (2020), https://doi.org/10.1016/j.mex.2019.10.036

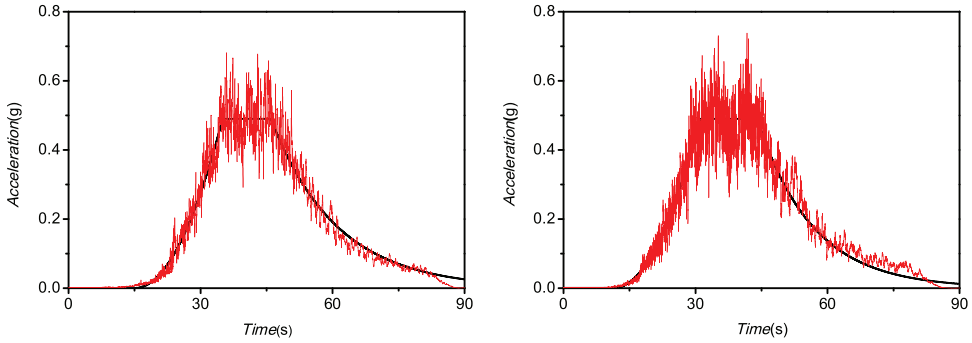

(a) the horizontal component (b) the vertical component

Fig. 3. The average absolute value.
(a) the horizontal component (b) the vertical component.

$$e(t) = \begin{cases} 1.0 \times 10^{-3} & 0 < t \le 12 \\ 1.3 \times 10^{-3}\left(t - 1.1 \times 10^{1}\right)^{2} & 12 < t \le 31 \\ 4.9 \times 10^{-1} & 31 < t \le 44 \\ e^{\left(-t \times 8.0 \times 10^{-2} + 2.8\right)} & 44 < t \le 90 \end{cases} \tag{3}$$

The first segment function in the formula is adjusted for matching the three segment model, not in the three segment model. In Fig. 3, it is found that the mean of the time-varying amplitude function is divided into three segments, and the difference between the time-varying amplitude function and the fitting function is also divided into three segments. The average standard deviation of each function is listed in Table 2. It is found that the distribution of time variable functions is approximately uniform distribution with $e(t)$ as the mean.

The Time-varying frequency function

After obtaining the time-varying amplitude function, the wavelet technique is used to obtain the time-varying frequency function of each record. The time-varying frequencies are obtained by the wavelet and the wavelet technique moves from the beginning to the end of the record. Then a series of wavelet coefficients are produced by continuous wavelet transform. According to the study [20], the frequency of the largest wavelet coefficient is considered as the main frequency of the record at that time and the frequency of the largest wavelet coefficient can be calculated by the scale of that coefficient.

Using this method, the time-varying frequency function of each record can be obtained. Because these ground motions are recorded in smaller area and the site conditions are similar, the ground motions can be considered to have the similar the time-varying frequency function. These time-varying frequency functions of these records can be represented by the average values. The average time-varying frequency function is shown as Fig. 4.

Table 2
Standard deviation of each segment.

	1	2	3	4
MSDH(g)	0.0029	0.0229	0.0540	0.0205
MSDV(g)	0.0012	0.0231	0.0572	0.0254

where MSDH represents the standard deviation of each segment of the horizontal time-varying amplitude function. MSDV represents the standard deviation of each segment of the vertical time-varying amplitude function.

Please cite this article in press as: Z. Liu, et al., A Multi Record Based Artificial Near Fault Ground Motion Generation Method, MethodsX (2020), https://doi.org/10.1016/j.mex.2019.10.036

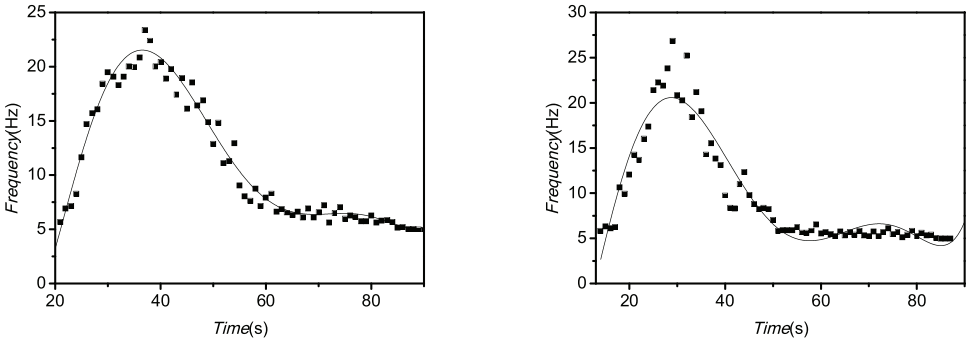

(a) the horizontal component (b) the vertical component

Fig. 4. Fitting of the time-varying frequency function for the horizontal components.

The amplitude of these ground motion records is quite small at the beginning of the record and the frequencies are hardly obtained using the wavelet transform. Because of these reasons, the frequencies of that part are replaced by the natural frequency of the site. The frequencies of the rest of the record are fitted by a suitable algebraic time function. According to studies [12,22], the high-order polynomial function is suggested to have a very good fit result. Then the time-varying frequency functions are shown as follows:

$$\omega_{gH}(t) = -2.68 \times 10^{-10} \times t^6 + 6.82 \times 10^{-8} \times t^5 - 6.18 \times 10^{-6} \times t^4 + 2.32 \times 10^{-4} \times t^3 - 3.00 \times 10^{-3} \times t^2 + 9.20 \times 10^{-3} \times t + 8.00 \times 10^{-3} \tag{4}$$

$$\omega_{gV}(t) = 1.43 \times 10^{-8} \times t^6 - 4.26 \times 10^{-6} \times t^5 + 4.83 \times 10^{-4} \times t^4 - 2.54 \times 10^{-2} \times t^3 - 5.90 \times 10^{-1} \times t^2 - 3.89 \times t - 5.10 \tag{5}$$

where the $\omega_{gH}(t)$ and $\omega_{gV}(t)$ are time-varying frequency functions of horizontal components and the vertical components, respectively.

The scaled stochastic acceleration record

The time-varying amplitude function and time-varying frequency function of these samples are obtained by using wavelet technology. Then the artificial ground motion model has obtained enough information of these samples to generate artificial ground motion.

The scaled stochastic acceleration record is obtained from the following formulas [23].

$$X_f^{\bullet\bullet}(t) + 2\xi_{(g)}\omega_{(g)}X_f^{\bullet}(t) + \omega_{(g)}^2 X_f(t) = n(t) \tag{6}$$

$$X_g^{\bullet\bullet}(t) = -\left(2\xi_{(g)}\omega_{(g)}X_f^{\bullet}(t) + \omega_{(g)}^2 X_f(t)\right) \tag{7}$$

where $X_f^{\bullet\bullet}$ is the filtered response; $X_g^{\bullet\bullet}$ is the output acceleration record; $\omega_{(g)}$ and $\xi_{(g)}$ are the frequency and the damping coefficient which are obtained from the ground motion record; $n(t)$ is a Gaussian white noise process.

$$E[n(t)] = 0 \tag{8}$$

Please cite this article in press as: Z. Liu, et al., A Multi Record Based Artificial Near Fault Ground Motion Generation Method, MethodsX (2020), https://doi.org/10.1016/j.mex.2019.10.036

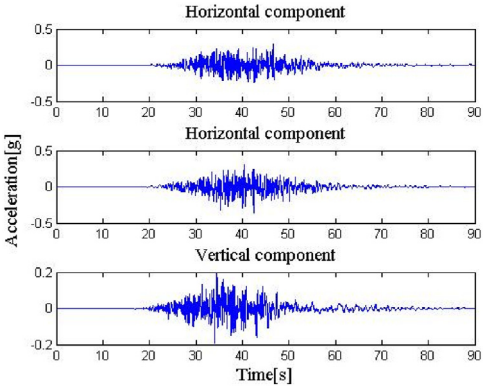

Fig. 5. Artificial ground motion.
(a) the plan of the steel frame (m) (b) the elevation of the steel frame (m).
(c) the cross section of the column (mm).
(d) the cross section of the beam (mm).

$$E[n(t_1)n(t_2)] = 2\pi G_o \delta(t_1 - t_2) \tag{9}$$

where *E[]* means the expected value; *δ()* is the Dirac delta function.

The scaled stochastic acceleration record is obtained using the formula above equ 5 and equ 6. The $\omega_g(t)$ is achieved from the continuous wavelet transform and $\xi_{(g)}$ is assumed to be 0.3 basing the previous works [12,22].

In order to illustrate the method of artificial ground motion generation, a simulation is carried out for each sample, and a total of 29 simulations are carried out. Using time-varying frequency function and damping function ratio, the artificial scaled stochastic acceleration records can be obtained.

After scaling the scaled stochastic acceleration record, the time-varying amplitude function is needed to obtain artificial acceleration. According to the probability distribution of the time-varying amplitude function, 29 time varying amplitude functions are obtained. Then the artificial stochastic acceleration record is generated basing the following formula.

$$a_r(t) = e(t; t_1, t_2, t_3) X_g^{\bullet\bullet}(t, \omega(t)) \tag{10}$$

where $a_r(t)$ is artificial stochastic acceleration record; $e(t; t_1; t_2; t_3)$ is the time-varying amplitude function which is obtained from the stochastic acceleration record; $\ddot{X}_g$ is the scaled stochastic acceleration record.

Artificial ground motion

After obtaining artificial stochastic acceleration record, it is necessary to continue adjustment to obtain artificial seismic waves. The two adjustment needs to be done. The first is to adjust the signal energy of the artificial stochastic acceleration record. When the amplitude function is acquired, the signal energy of each sample is adjusted to the same value. In simulation, it is necessary to adjust the energy of artificial stochastic acceleration record to the energy of its earthquake sample. The second is to add near fault velocity pulse. The artificial near fault ground motion is generated by adding the corresponding near fault velocity pulse in the artificial seismic wave. For example, artificial seismic waves generated from a sample are added to the velocity pulses extracted from this sample and the sample is shown as Fig. 5. So as to ensure the authenticity of artificial near fault ground motion.

Please cite this article in press as: Z. Liu, et al., A Multi Record Based Artificial Near Fault Ground Motion Generation Method, MethodsX (2020), https://doi.org/10.1016/j.mex.2019.10.036

Table 3
Detailed parameters of the six-storied steel frame.

parameter	L	W	H	T	E_{steel}	F_{steel}
value	5	3	6	22t	206GPa	345MPa

where L is the number of span in the length direction of the steel frame; W is the number of span in the width direction of the steel frame; H is the layer number of the steel frame; T is the node average added mass in order to simulate the floor and the wall mass; E_{steel} and F_{steel} are the elastic modulus and yield strength of the steel used in the steel frame, separately.

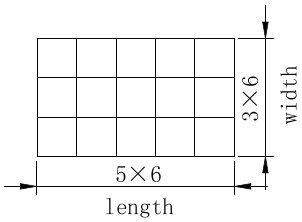

(a) the plan of the steel frame (m)

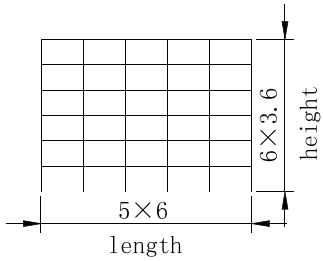

(b) the elevation of the steel frame (m)

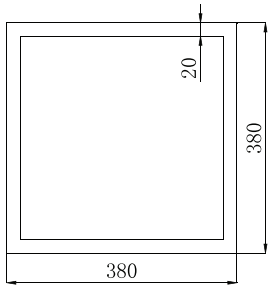

(c) the cross section of the column (mm)

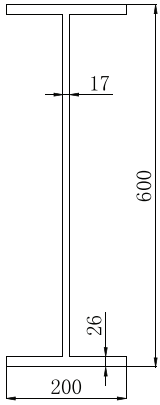

(d) the cross section of the beam (mm)

Fig. 6. Dimension diagram of steel frame.
(a) horizontal component (b) the vertical component.

Please cite this article in press as: Z. Liu, et al., A Multi Record Based Artificial Near Fault Ground Motion Generation Method, MethodsX (2020), https://doi.org/10.1016/j.mex.2019.10.036

The evaluation of artificial ground motions

Using this method, 29 artificial near fault ground motions are obtained. Because these artificial ground motions are generated basing a set of actual ground motions, the usual evaluation methods do not fit these artificial ground motions. In order to evaluation these artificial ground motions, a steel frame is modeled in finite element analysis program (ANSYS). If the two ground motions produce the same displacement of the steel frame, two ground motions are considered to have the same structural damage. If the actual ground motion and the artificial ground motion which generated from this actual ground motion have the same structural damage, the artificial ground motion is considered as a good simulation of this actual ground motion. The same rule can be used in a set of ground motions.

According to the building seismic code of China, the six-story steel frame structure is designed and detailed parameters of the six-story steel frame structure are shown as Table 3, Figs. 6 and 7.

In order to ensure the seismic capacity, the strong column weak beam system is used, and the joints of beam column and column base are rigid. The connection node of column and beam is as shown in the Fig. 7. The site type of the structure is relatively hard rock site. The seismic fortification intensity of the structure is 8 degrees. ANSYS finite element program is used to model the frame structure. Column and beam are simulated by beam 188 element and node mass is simulated by mass21 element.

These actual ground motions and these artificial ground motions are input to this steel frame, respectively. Then displacements are obtained. According to the work [24], the relationship between the structural displacement and the earthquake parameters is considered to be linear in log-log coordinate. The relationships between the structural displacement and the energy of ground motion are shown in Figs. 7 and 8.

From the Figs. 8 and 9, it can be found that the seismic damage of ground motion with velocity pulse is significantly higher than the corresponding residual ground motion. This shows that the velocity pulse has a significant effect on damage. It can also be found that the formulas which obtained from artificial ground motions have almost the same coefficients as the formulas of actual ground motions. The biggest difference exists in the formulas of the horizontal components. The small number of actual ground motions and the velocity pulses may be a reason for this. Then a conclusion can be made that these artificial near-fault ground motions are good simulations of these actual ground motions. Because the velocity pulse is added to artificial ground motion, the artificial ground motion can be considered to have the same structural damage as the actual ground motion. This method is enough precision to generate the near-fault ground motion which is used in the engineering field. The great advantage of this method is that the ground motion can be generated basing a set of actual ground motions. Artificial seismic ground motion generated by artificial ground motion generation method based on multiple records can reflect earthquake characteristics. Compared with

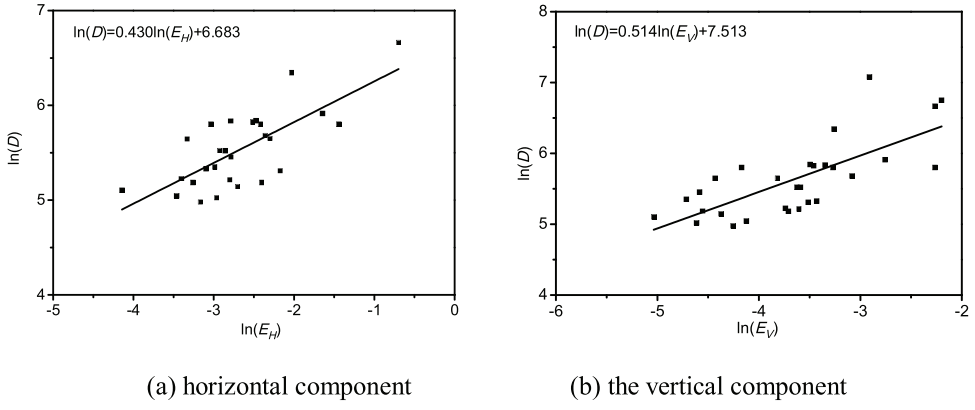

Fig. 7. The relationship basing actual ground motions.
(a) horizontal component (b) the vertical component.

Please cite this article in press as: Z. Liu, et al., A Multi Record Based Artificial Near Fault Ground Motion Generation Method, MethodsX (2020), https://doi.org/10.1016/j.mex.2019.10.036

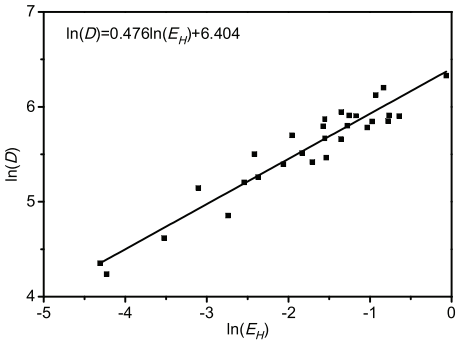

(a) horizontal component

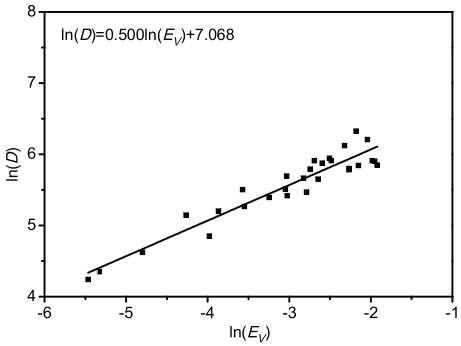

(b) the vertical component

Fig. 8. The relationship basing artificial ground motions.
(a) the horizontal component (b) the vertical component.
(c) the residual component.

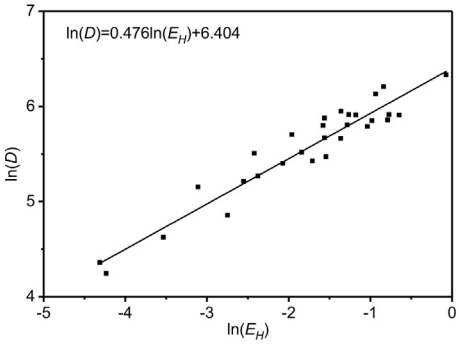

(a) the horizontal component

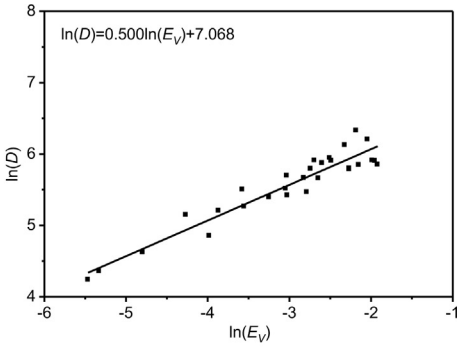

(b) the vertical component

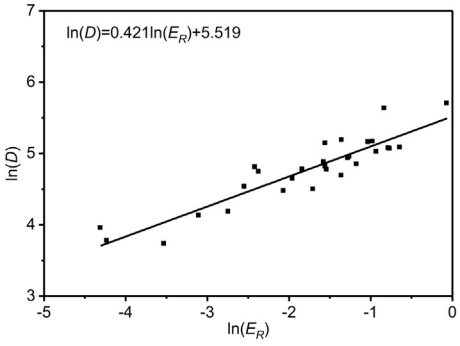

(c) the residual component

Fig. 9. The relationship basing artificial ground motions.

Please cite this article in press as: Z. Liu, et al., A Multi Record Based Artificial Near Fault Ground Motion Generation Method, MethodsX (2020), https://doi.org/10.1016/j.mex.2019.10.036

other artificial ground motion generation methods based on a single ground motion, the artificial seismic ground motion method based on multiple ground motions can take into account the uncertainty of each sample under the premise of considering the overall earthquake characteristics. So as to produce artificial seismic waves better

Conclusions

In this paper, a method of near fault ground motion generation based on multiple ground motions is proposed. In this method, the wavelet technique is used to obtain the time-varying amplitude function and the time-varying frequency function of the ground motions, and the artificial ground motion is generated by using two functions. In the process of generating seismic waves, the overall characteristics of earthquake are fully taken into account, and the variability of various ground motions is reasonably taken into account. So that the simulated seismic waves are closer to the characteristics of natural seismic waves. A steel frame is modeled in finite element analysis program to evaluate the artificial near-fault ground motions. In comparison with the actual ground motions, the artificial ground motions cause the same structural damage. The artificial near-fault ground motion can be considered as a good simulation of original ground motion.

Acknowledgments

This work is supported by the National Natural Science Foundation Key Project of China (No. 51178080). The author would like to thank the Pacific Earthquake Engineering Research Center for the earthquake data.

References

[1] K. Yazdannejad, A. Yazdani, Prediction of seismic demand model for pulse like ground motions using artificial neural networks, Canadian Journal of Civil Engineering 44 (2017) 0043.
[2] S. Yaghmaei-Sabegh, M. Ebrahimi-Aghabagher, Near-field probabilistic seismic hazard analysis with characteristic earthquake effects, Natural Hazards 87 (3) (2017) 1607–1633.
[3] J.D. Bray, A. Rodriguez-Marek, Characterization of forward-directivity ground motions in the near-fault region, Soil Dynamics & Earthquake Engineering 24 (2004) 815–828.
[4] M. Fathi, A. Makhdoumi, M. Parvizi, Effect of supplemental damping on seismic response of base isolated frames under near & far field accelerations, Ksce Journal of Civil Engineering 19 (2015) 1359–1365.
[5] D. Yang, J. Pan, G. Li, Non-structure-specific intensity measure parameters and characteristic period of near-fault ground motions, Earthquake Engineering & Structural Dynamics 38 (2010) 1257–1280.
[6] G.P. Mavroeidis, G. Dong, A.S. Papageorgiou, Near-fault ground motions, and the response of elastic and inelastic single-degree-of-freedom (SDOF) systems, Earthquake Engineering & Structural Dynamics 33 (2004) 1023–1049.
[7] X. Huang, S. Hou, M. Liao, Z. Zhu, Bearing capacity evaluation and reinforcement analysis of bridge piles under strong earthquake conditions, Ksce Journal of Civil Engineering (2017) 1–9.
[8] M. Torbol, Quasi real-time post-earthquake damage assessment of lifeline systems based on available intensity measure maps, Smart Structures & Systems 16 (2015) 873–889.
[9] M.R. Shiravand, A.K. Nejad, M.H. Bayanifar, Seismic response of RC structures rehabilitated with SMA under near-field earthquakes, Structural Engineering & Mechanics 63 (2017) 497–507.
[10] H. Tajammolian, F. Khoshnoudian, V. Bokaeian, Seismic responses of asymmetric steel structures isolated with the TCFP subjected to mathematical near-fault pulse models, Smart Structures And Systems 15 (2016) 931–953.
[11] T.C. Shin, "A Preliminary Report on the 1999 Chi-Chi (Taiwan) Earthquake", Seismological Research Letters 71 (1999) 24–30.
[12] J.W. Baker, Quantitative Classification of Near-Fault Ground Motions Using Wavelet Analysis, Bulletin of the Seismological Society of America 97 (2007) 1486–1501.
[13] S. Yaghmaei-Sabegh, Detection of pulse-like ground motions based on continues wavelet transform, Journal of seismology 14 (2010) 715–726.
[14] P. Mimoglou, I.N. Psycharis, I.M. Taflampas, Explicit determination of the pulse inherent in pulse-like ground motions, Earthquake Engng Struct. Dyn 43 (2014) 2261–2281.
[15] K. Kanai, Semi-empirical Formula for the Seismic Characteristics of the Ground, Sci Res. 35 (1957).
[16] H. Tajimi, A statistical method of determining the maximum response of a building structure during an earthquake, Proceedings from the 2nd World Conference on Earthquake Engineering, Japan (1960) 781–798.
[17] P. Cacciola, I. Zentner, Generation of response-spectrum-compatible artificial earthquake accelerograms with random joint time–frequency distributions, Probabilistic Engineering Mechanics 28 (2012) 52–58.
[18] F.G. Fan, G. Ahmadi, Nonstationary Kanai-Tajimi Models for El Centro 1940 and Mexico City 1985 Earthquakes, Probabilistic Engineering Mechanics 5 (1990) 171–181.
[19] F. Naeim, M. Lew, On the Use of Design Spectrum Compatible Time Histories, Earthquake Spectra 11 (1995) 111–127.

Please cite this article in press as: Z. Liu, et al., A Multi Record Based Artificial Near Fault Ground Motion Generation Method, MethodsX (2020), https://doi.org/10.1016/j.mex.2019.10.036

[20] G.G. Amiri, A.A. Rad, N.K. Hazaveh, Wavelet-Based Method for Generating Nonstationary Artificial Pulse-Like Near-Fault Ground Motions, Computer-Aided Civil and Infrastructure Engineering 29 (2015) 758–770.
[21] S.S. Yaghmaei, Stochastic finite fault modeling for the 16 September 1978 Tabas, Iran, earthquake, IJE Transactions A: Basics 24 (1) (2011) January 2011.
[22] B.W. Dickinson, H.P. Gavin, Parametric Statistical Generalization of Uniform-Hazard Earthquake Ground Motions, Journal of Structural Engineering 137 (2011) 410–422.
[23] F.R. Rofooei, A. Mobarake, G. Ahmadi, Generation of artificial earthquake records with a nonstationary Kanai–Tajimi model, Engineering Structures 23 (2001) 827–837.
[24] Y. Pan, A.K. Agrawal, M. Ghosn, Seismic Fragility of Continuous Steel Highway Bridges in New York State, Journal of Bridge Engineering 12 (2007) 689–699.

Please cite this article in press as: Z. Liu, et al., A Multi Record Based Artificial Near Fault Ground Motion Generation Method, MethodsX (2020), https://doi.org/10.1016/j.mex.2019.10.036